Nonperturbative approach for the electronic Casimir-Polder effect in a one-dimensional semiconductor

Satoshi Tanaka,[1,*] Roberto Passante,[2] Taku Fukuta,[1] and Tomio Petrosky[3]

[1]*Department of Physical Science, Osaka Prefecture University, Gakuen-cho 1-1, Sakai 599-8531, Japan*

[2]*Dipartimento di Fisica e Chimica dell' Università degli Studi di Palermo and CNISM, Via Archirafi 36, I-90123 Palermo, Italy*

[3]*Center for Studies in Statistical Mechanics and Complex Systems, The University of Texas at Austin, Austin, Texas 78712, USA*

(Received 22 April 2013; published 27 August 2013)

We present the electronic Casimir-Polder effect for a system consisting of two impurities on a one-dimensional semiconductor quantum wire. Due to the charge transfer from the impurity to a one-dimensional conduction band, the impurity states are dressed by a virtual cloud of the electron field. The attractive electronic Casimir force arises due to the overlap of the virtual clouds. The Van Hove singularity causes the persistent bound state (PBS) to appear below the band edge even when the bare impurity state energy is above the band edge. Since the decay rate of the virtual cloud of the PBS in space is small, the Casimir force can be of a very long range. While the overlap of the electronic virtual cloud is consistent with the idea of the radiation reaction, it is shown that also vacuum fluctuations play a role in the electronic Casimir force as a result of the fermionic anticommutation relations. We introduce an effective mass, different from the effective band mass of the conduction band, which is associated with the distance of the energy of the PBS from the band edge where the Van Hove singularity is located and determines the decay rate of the electronic Casimir-Polder force.

DOI: 10.1103/PhysRevA.88.022518 PACS number(s): 31.30.jh, 12.20.Ds, 73.20.−r, 73.21.Hb

I. INTRODUCTION

Dressing is a fundamental phenomenon of quantum field theory. Every quantum particle is dressed by virtual quanta through an interaction with a quantum field. It has been recognized that mass renormalization and damping are accompanied with this dressing process. They are represented, respectively, by the real part and the imaginary part of the self-energy of a quasiparticle interacting with a field. The Casimir effect [1] predicted by Casimir in 1948 is one of the typical examples of dressing processes, and its related phenomena have been extended to vast areas of physics, such as elementary particle physics, cosmology, quantum optics, chemical physics, nanotechnology, and biology [2–5].

In the Casimir effect, two neutral bodies in their ground state attract each other by coupling to the electromagnetic vacuum field. The Casimir effect is profound because it clearly reveals the presence of the virtual quanta of a field even in the ground state of the source-field system, despite that one would expect that the lowest possible state of a source coupled to a field should be devoid of quanta of radiation. A ground-state source interacts with a vacuum field by virtual transitions, which give rise to a virtual cloud around the source, and the overlap of the virtual clouds causes the Casimir force on the sources.[1]

While the Casimir effect has been traditionally explained by a perturbative approach [6,7], there are many systems in which a perturbative analysis is inappropriate. As an example, when the coupling of a source with a field becomes strong, nonperturbative effects must be taken into account, as in photonic crystals where interesting radiative effects arise due to the strong coupling, such as giant Lamb shift and enhanced spontaneous decay [8–10]. A nonperturbative method is required to study the electronic Casimir effect of the present one-dimensional system, since there is the Van Hove singularity in the density of states of the one-dimensional conduction band [11–13]. Due to the divergence of the density of states at the band edge, the coupling strength of the atom with the field becomes enormously strong, which prevents us from using a perturbative analysis. We have recently found the nonanalytic decay rate of an unstable particle embedded in a one-dimensional semiconductor as an example of a peculiar feature due to the Van Hove singularity [12].

Even in the weak coupling, when one studies the Casimir-Polder effect in an excited state, perturbative methods break down due to the resonant singularity [14–18]. Therefore it is necessary to develop nonperturbative methods in order to study Casimir effects in these various systems.

Recently, nonperturbative methods for dressed states of the electromagnetic field have been developed [19,20]. We have derived an exact expression of the atom-atom and atom-surface Casimir-Polder interaction energy with a nonperturbative method which uses Bogolioubov-type transformations [21,22]. Then it is important to reveal characteristic features of nonperturbative effects of Casimir forces in various systems.

In this work we study a Casimir effect in a pure electronic system of a one-dimensional semiconductor with two impurity atoms. An attractive force appears between the two impurity atoms due to an overlap of the virtual cloud of free electrons around the impurity atoms, which is equivalent to the mechanism of the electromagnetic Casimir force where the virtual photon clouds surrounding neutral atoms overlap each other. A characteristic feature of the electronic Casimir effect is seen in the distance dependence of the force: The electronic Casimir force decreases exponentially with the distance, while it decreases with a power law in the electromagnetic case. This difference is attributed to a finite effective mass of the

*stanaka@p.s.cias.osakafu-u.ac.jp

[1]In a strict manner, we should call the present system as a Casimir-Polder effect since the bodies are microscopic objects, such as atoms. However, in the present paper, we may refer to the attractive interaction of the impurity atoms as Casimir effect, for simplicity.

electronic field, while the radiation field is a massless field. Then the electronic Casimir force is to be compared to the attractive nuclear force described by the Yukawa potential, which is caused by the exchange of a relativistic massive meson field [6,7].

One of the striking features of the Van Hove singularity is an appearance of the bound state just below the band edge regardless of the bare impurity energy [12,13,23]: We call this bound state *persistent bound state* (PBS), which cannot be described by a usual perturbation method. In the present work we find that the tail of the virtual cloud in the PBS extends to a long distance with a very small exponential decay rate. Therefore the attractive force works between the two impurity atoms even when they are separated by a long distance. On the other hand, for a short distance, the electronic Casimir force does not follow the exponential law.

As for the physical understanding of the Casimir effect, two alternative interpretations have been presented for the electromagnetic Casimir effect: One is the radiation reaction and the other is the vacuum fluctuations. In the picture of the radiation reaction, the zero-point field is a superfluous concept, and the Casimir effect is attributed to the interaction of the atom with the field which the other atom creates. On the other hand, in the picture of vacuum fluctuations, the zero-point field plays an essential role, where the antinormal ordering of the field operators in the vacuum state gives vacuum fluctuations. The interaction energy is influenced by the presence of vacuum fluctuations. Although these two interpretations look qualitatively different, Milonni *et al*. revealed that they are two sides of the same coin about the Casimir effect [6,7,24,25].

In this work, however, we emphasize that the electronic Casimir-Polder effect is interpreted in terms of the radiation reaction field, where one of the two sources creates a virtual cloud of the field around itself, and the interaction of this field with the other atom induces the Casimir-Polder energy which is the origin of the Casimir-Polder force. There is no need to utilize the idea of vacuum fluctuations of the field as a cause of the electronic Casimir-Poder effect.

In Sec. II we present a model system which consists of the one-dimensional semiconductor on which two neutral impurity atoms are separately placed. The charge transfer between the impurity and the semiconductor substrate is taken into account. The dressed ground state of the complete system (impurity atoms + field) is obtained in Sec. III using a nonperturbative method.

In Sec. IV the electronic Casimir energy is evaluated and we show that the Casimir energy becomes a long-range force with a very small decay rate for the PBS. It is found that the spatial extension of the electronic Casimir force of an adsorbed atom on the silicon semiconductor reaches to a few hundred Angstrom.

In Sec. V we show that the electronic Casimir-Polder effect can be interpreted in line with the thought of the radiation reaction. It is clear for a boson field that the Casimir effect does not require the vacuum fluctuations, because the boson field can be translated to a classical field with use of the correspondence of the commutation relation to the Poisson bracket. In the present case, however, since there is no clear correspondence between the fermion field and a classical field, we see that vacuum fluctuations play a role in the antinormal ordering of the field operators. In Sec. V we then introduce an effective fermion field which can be compared with the relativistic massive scalar field, and define a new effective mass, different from the effective band mass of the conduction electron. We give a summary in Sec. VI.

II. MODEL

We shall consider a system where two neutral impurity atoms, e.g., $Na^0(^2S_{1/2})$ and $I^0(^2P_{3/2})$, are placed on a one-dimensional semiconductor wire at $x = 0$ and $x = R$, respectively, as shown in Fig. 1(a). In Fig. 1(b) we show the energy scheme of the semiconductor band structure and the impurity states, where the bare energies of the outermost shell of the impurities fall in the energy gap between the valence and the conduction bands. In the present work we assume that the bare energies of the impurities are close to the conduction band so that we neglect the interaction between the impurity states and the valence band.

In the study of the Casimir effect, it is important to distinguish between a source system and a continuous field in order to clarify the role of the vacuum field. In the present work we recognize the two impurity atoms as a source system and the semiconductor conduction band as a continuous field.

The source system is described by

$$\hat{H}_A = \varepsilon_1 d_1^\dagger d_1 + \varepsilon_2 d_2^\dagger d_2, \tag{1}$$

where the first and second terms represent the impurity states at $x = 0$ and $x = R$, respectively, with energies ε_1 and ε_2. The operators d_i and $d_i^\dagger$ $(i = 1,2)$ are electron annihilation and creation operators for the impurity states.

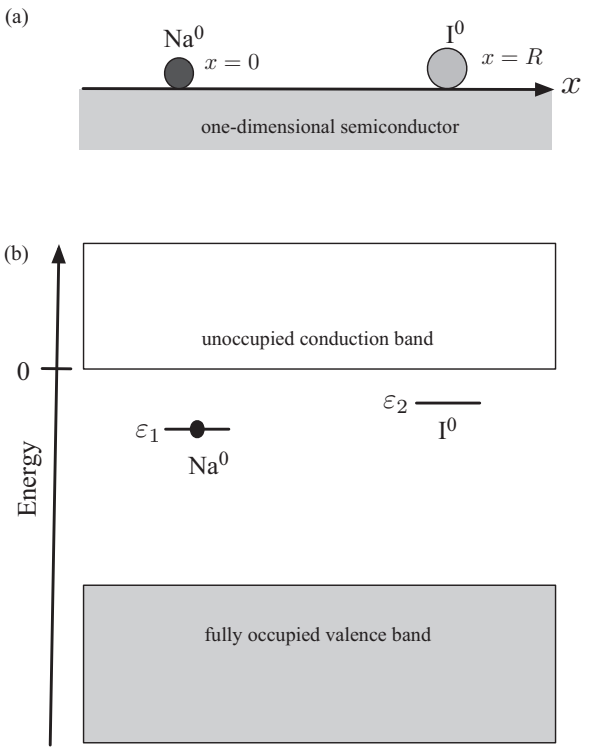

FIG. 1. Two impurity atoms with their outermost energy levels embedded in the energy gap of a one-dimensional semiconductor.

The eigenstates of $\hat{H}_A$ are described by (one-electron subspace)

$$|d_i\rangle_A = d_i^\dagger|0\rangle_A \quad (i = 1,2), \tag{2}$$

with the eigenenergies ε_i, where $|0\rangle_A$ is an electron vacuum of the impurity system defined by

$$d_i|0\rangle_A = 0 \quad \text{for} \quad i = 1,2. \tag{3}$$

The field Hamiltonian of the one-dimensional conduction band is written as

$$\hat{H}_F = \sum_k \varepsilon_k a_k^\dagger a_k, \tag{4}$$

where a_k and $a_k^\dagger$ are the conduction band electron operators that satisfy anticommutation relations. In Eq. (4) we take the free electron energy dispersion relation

$$\varepsilon_k = \frac{\hbar^2 k^2}{2m_e}, \tag{5}$$

with an effective conduction band mass m_e. The lowest band edge of the conduction band is taken to be the energy origin, as shown in Fig. 1(b). The wave number k represents a normal mode of the free electron field. By imposing the usual periodic boundary conditions, the wave number is discretized as

$$k_j = \frac{2\pi j}{L} \quad (j = \text{integer}), \tag{6}$$

where L is the length of the system. The wave function with a wave number k is given by

$$\psi_k(x) \equiv \langle x|k\rangle = \frac{1}{\sqrt{L}} e^{ikx}. \tag{7}$$

In the limit of large length $L \to \infty$, we have

$$\frac{1}{\Omega}\sum_j \to \int dk, \quad \Omega\delta_{k,k'}^{Kr} \to \delta(k-k'), \tag{8}$$

where $\Omega \equiv L/2\pi$.

The vacuum state $|\{0_k\}\rangle_F$ of the field satisfies

$$a_k|\{0_k\}\rangle_F = 0, \quad \text{for} \quad \forall k. \tag{9}$$

The zero-point energy of the bare vacuum state is given by

$$E_0 = {}_F\langle\{0_k\}|\hat{H}_F|\{0_k\}\rangle_F = 0. \tag{10}$$

A conduction electron with a wave number k created from the vacuum field $|\{0_k\}\rangle_F$ is given by

$$|1_k,\{0\}'\rangle_F \equiv a_k^\dagger|\{0_k\}\rangle_F, \tag{11}$$

where $|\{0\}'\rangle$ denotes a direct product of the states of all normal modes except a mode k. The state $|1_k,\{0\}'\rangle_F$ is an eigenstate of $\hat{H}_F$ with the energy ε_k:

$$\hat{H}_F|1_k,\{0\}'\rangle_F = \varepsilon_k|1_k,\{0\}'\rangle_F. \tag{12}$$

For simplicity we shall write the vacuum state $|\{0_k\}\rangle_F$ and the state $|1_k,\{0\}'\rangle_F$ by $|0\rangle_F$ and $|1_k\rangle_F$, respectively.

We consider that the source-field interaction is attributed to the charge transfer interaction between the impurity atoms and the conduction band which is represented by

$$\hat{H}_{AF} = g_1\hat{V}_1 + g_2\hat{V}_2 \tag{13a}$$

$$= g_1\sum_k (V_{1k}a_k^\dagger d_1 + V_{1k}^* d_1^\dagger a_k) + g_2\sum_k (V_{2k}a_k^\dagger d_2 + V_{2k}^* d_2^\dagger a_k), \tag{13b}$$

where g_1 and g_2 are dimensionless coupling constants. When we assume a point interaction at the position of the impurity, the interaction potentials of V_{1k} and V_{2k} are represented by

$$V_{1k} = V_{1k}^* = V, \tag{14a}$$

$$V_{2k} = Ve^{ikR}, \quad V_{2k}^* = Ve^{-ikR}, \tag{14b}$$

where g_1 and g_2 are the dimensionless coupling constants. In this work we take V as an energy unit. We further denote

$$v \equiv \frac{V}{\sqrt{\Omega}}. \tag{15}$$

The total Hamiltonian is the sum of $\hat{H}_A$, $\hat{H}_F$, and $\hat{H}_{AF}$,

$$\hat{H} = \hat{H}_A + \hat{H}_F + H_{AF}. \tag{16}$$

In the present work we consider a single electron vector space which is spanned by a basis set of the total source-field system:

$$|d_1;0\rangle \equiv |d_1\rangle_A \otimes |0\rangle_F, \tag{17a}$$

$$|d_2;0\rangle \equiv |d_2\rangle_A \otimes |0\rangle_F, \tag{17b}$$

$$|0;k\rangle \equiv |0\rangle_A \otimes |1_k\rangle_F, \tag{17c}$$

where the atomic states $|\alpha\rangle_A$ ($\alpha = d_1,d_2,0$) and the field state $|\beta\rangle_F$ ($\beta = 0,1_k$) are defined above. In terms of the vector space generated by $\{|d_1;0\rangle,|d_2;0\rangle,|0;1_k\rangle\}$, the Hamiltonian is represented by

$$\hat{H} = \varepsilon_1|d_1;0\rangle\langle d_1;0| + \varepsilon_2|d_2;0\rangle\langle d_2;0| + \sum_k \varepsilon_k|0;k\rangle\langle 0;k| + \frac{g_1 v}{\sqrt{\Omega}}\sum_k (|0;k\rangle\langle d_1;0| + |d_1;0\rangle\langle 0;k|) + \frac{g_2 v}{\sqrt{\Omega}}\sum_k (e^{ikR}|0;k\rangle\langle d_2;0| + e^{-ikR}|d_2;0\rangle\langle 0;k|), \tag{18}$$

which is of the same form as the two-level Friedrichs model [26]. This type of Hamiltonian, known as Newns-Anderson Hamiltonian, has been extensively used to describe the adsorption of an atom on a surface [27,28].

In the next section we solve the eigenvalue problem of the Hamiltonian given by Eq. (18), and obtain the true (interacting) vacuum state for our system. The Casimir-Polder force is obtained by taking a negative derivative of the renormalized vacuum energy as a function of R.

In this paper we adopt the following notations according to Ref. [29]. By dividing the eigenvalue problem of $\hat{H}$ by $\hbar^2/2m$, we consider the eigenvalue problem

$$\tilde{H}|\phi_0\rangle = \zeta|\phi_0\rangle, \tag{19}$$

with

$$\tilde{H} = \tilde{H}_A + \tilde{H}_F + \tilde{H}_{AF}, \tag{20}$$

where

$$\tilde{H}_A = \zeta_1 |d_1;0\rangle\langle d_1;0| + \zeta_2 |d_2;0\rangle\langle d_2;0|, \tag{21a}$$

$$\tilde{H}_F = \sum_k \zeta_k |0;k\rangle\langle 0;k|, \tag{21b}$$

$$\tilde{H}_{AF} = g_1\tilde{V}_1 + g_2\tilde{V}_2 \tag{21c}$$

$$= \frac{g_1 u}{\sqrt{\Omega}} \sum_k (|0;k\rangle\langle d_1;0| + |d_1;0\rangle\langle 0;k|) + \frac{g_2 u}{\sqrt{\Omega}} \sum_k (e^{ikR}|0;k\rangle\langle d_2;0| + e^{-ikR}|d_2;0\rangle\langle 0;k|). \tag{21d}$$

In Eqs. (21) we denote

$$\zeta_j \equiv \frac{\varepsilon_j}{\hbar^2/2m_e} \quad (j = 1,2); \quad u \equiv \frac{v}{\hbar^2/2m_e}, \quad \zeta_k \equiv k^2. \tag{22}$$

Note that the dimension of these variables are $[\zeta] = [L^{-2}]$ and $[u] = [L^{-3/2}]$. Corresponding to the energy unit V, we take the length unit as

$$l_0 \equiv \left(\frac{\hbar^2/2m_e}{V}\right)^{1/2}. \tag{23}$$

As an example, when we take the effective mass of silicon as $m_e = 0.16m_0$, where m_0 is a bare electron mass, and $V = 1$ eV for a typical charge transfer energy, the unit of length is estimated to be $l_0 = 4.9$ Å.

III. DRESSED QUANTUM VACUUM STATE

In this section we obtain the dressed ground state of the Hamiltonian H given by Eq. (18) by using a projection method outlined in Appendix A [30–33]. The dressed ground state $|\phi_0\rangle$ is obtained as the lowest-energy state of the solutions of

$$\tilde{H}|\phi_0\rangle = \zeta_g|\phi_0\rangle, \tag{24}$$

where ζ_g is a negative real number. We consider the projection operator onto the field vacuum state $|0\rangle_F$:

$$\hat{P}^{(d,0)} \equiv |d_1;0\rangle\langle d_1;0| + |d_2;0\rangle\langle d_2;0| = (|d_1\rangle\langle d_1| + |d_2\rangle\langle d_2|)_A \otimes |0\rangle\langle 0|_F. \tag{25}$$

As shown in Eq. (A9), the $\hat{P}^{(d,0)}$ component of $|\phi_0\rangle$ is obtained by solving the eigenvalue problem of the self-energy operator $\hat{\Xi}(z)$:

$$\hat{\Xi}(\zeta_g)|u_0\rangle = \zeta_g|u_0\rangle, \tag{26}$$

where $|u_0\rangle$ is a normalized eigenstate of $\hat{\Xi}(\zeta_g)$ defined by

$$|u_0\rangle \equiv \mathcal{N}_0^{-1/2}\hat{P}|\phi_0\rangle. \tag{27}$$

In Eq. (26) the components of the self-energy operator are represented in terms of the discrete state basis of Eqs. (17a) and (17b) as

$$\Xi_{11}(\zeta) \equiv \langle d_1;0|\hat{\Xi}(z)|d_1;0\rangle = \zeta_1 + \frac{g^2u_1^2}{\Omega}\sum_k \frac{1}{(\zeta-\zeta_k)^+}, \tag{28a}$$

$$\Xi_{21}(\zeta) \equiv \langle d_2;0|\hat{\Xi}(\zeta)|d_1;0\rangle = \frac{g^2u_1u_2}{\Omega}\sum_k \frac{e^{-ikR}}{(\zeta-\zeta_k)^+}, \tag{28b}$$

$$\Xi_{12}(\zeta) \equiv \langle d_1;0|\hat{\Xi}(\zeta)|d_2;0\rangle = \frac{g^2u_1u_2}{\Omega}\sum_k \frac{e^{ikR}}{(\zeta-\zeta_k)^+}, \tag{28c}$$

$$\Xi_{22}(\zeta) \equiv \langle d_2;0|\hat{\Xi}(\zeta)|d_2;0\rangle = \zeta_2 + \frac{g^2u_1^2}{\Omega}\sum_k \frac{1}{(\zeta-\zeta_k)^+}. \tag{28d}$$

The summations on k in Eqs. (28) reduce to Cauchy integrals in the large volume limit, which are evaluated as

$$\frac{g^2u_1^2}{\Omega}\sum_k \frac{1}{(\zeta-\zeta_k)^+} = g^2u_1^2\int_{-\infty}^{\infty}\frac{dk}{\zeta_+-\zeta_k} = -g^2v_1^2\frac{i\pi}{\sqrt{\zeta_+}}, \tag{29a}$$

$$\frac{g^2u_1u_2}{\Omega}\sum_k \frac{e^{ikR}}{(\zeta-\zeta_k)^+} = g^2u_1u_2\int_{-\infty}^{\infty}\frac{e^{ikR}}{\zeta_+-\zeta_k}dk = -g^2u_1u_2\frac{i\pi\exp(i\sqrt{\zeta_+}R)}{\sqrt{\zeta_+}}, \tag{29b}$$

where the "+" sign denotes the direction of the analytic continuation from the upper half of the complex ζ plane.

As seen in Eqs. (29), we find a divergence in the self-energies at the band edge $\zeta = 0$ due to the Van Hove singularity. As an example, we show in Figs. 2(a) and 2(b) the real and the imaginary parts of the self-energy $\Xi_{12}(\zeta')$ for $R = 10$, respectively, as a function of $\zeta' \equiv \mathrm{Re}(\zeta)$, where $g = 0.1$.

Then the eigenvalue problem of Eq. (26) is represented in terms of the discrete basis as

$$\begin{pmatrix} \Xi_{11}(\zeta_g) & \Xi_{12}(\zeta_g) \\ \Xi_{21}(\zeta_g) & \Xi_{22}(\zeta_g) \end{pmatrix}\begin{pmatrix}\beta_1\\ \beta_2\end{pmatrix} = \zeta_g\begin{pmatrix}\beta_1\\ \beta_2\end{pmatrix}, \tag{30}$$

where

$$\beta_1 \equiv \langle d_1;0|u_0\rangle, \quad \beta_2 \equiv \langle d_2;0|u_0\rangle, \tag{31}$$

which are determined under the condition

$$\beta_1^2 + \beta_2^2 = 1. \tag{32}$$

From Eq. (30) we have

$$\frac{\beta_2}{\beta_1} = -\frac{\Xi_{11}-\zeta_g}{\Xi_{12}}, \tag{33}$$

and with (32) we have

$$\beta_1 = \left[1 + \frac{(\Xi_{11}-\zeta_g)^2}{\Xi_{12}^2}\right]^{-\frac{1}{2}}. \tag{34}$$

The dressed ground-state energy ζ_g is then obtained as the lowest energy solution of the characteristic equation of

$$\begin{vmatrix} \Xi_{11}(\zeta_g)-\zeta_g & \Xi_{12}(\zeta_g) \\ \Xi_{12}(\zeta_g) & \Xi_{22}(\zeta_g)-\zeta_g \end{vmatrix} = 0. \tag{35}$$

The wave function of the dressed ground state is obtained by adding the $\hat{Q}$ component to the $\hat{P}$ component as shown in

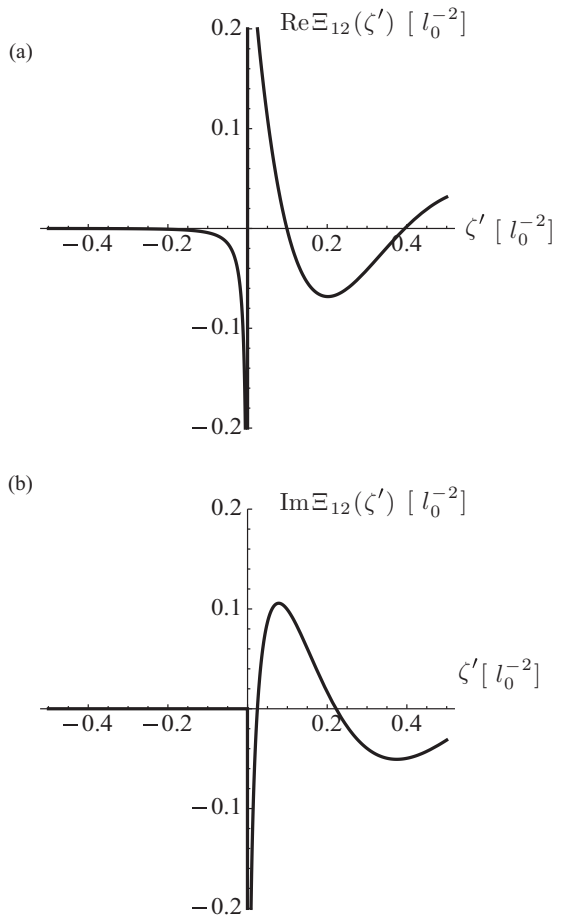

FIG. 2. The (a) real and (b) imaginary parts of $\Xi_{12}(\zeta')$ for $R = 10$, with $g = 0.1$, where $\zeta' \equiv \mathrm{Re}[\zeta]$, where l_0 is a length unit given in Eq. (23).

Eq. (A13):

$$|\phi_0\rangle = \mathcal{N}_0^{1/2}\{|u_0\rangle + \hat{Q}\hat{\mathcal{C}}(\zeta_g)|u_0\rangle\} \tag{36a}$$

$$= \mathcal{N}_0^{1/2}\left\{|d_1;0\rangle\beta_1 + |d_2;0\rangle\beta_2 + \frac{1}{\sqrt{\Omega}}\sum_k \frac{u}{\zeta_g - \zeta_k}(g_1\beta_1 + g_2 e^{ikR}\beta_2)|0;k\rangle\right\}, \tag{36b}$$

where β_1 and β_2 are given in Eqs. (33) and (34). In Eqs. (36) the normalization constant $\mathcal{N}_0$ is determined by

$$1 = \langle\phi_0|\phi_0\rangle = \mathcal{N}_0\left\{1 - \frac{\partial}{\partial\zeta}\left[\Xi_{11}(\zeta)\beta_1^2 + \Xi_{22}(\zeta)\beta_2^2 + \Xi_{12}(\zeta)\beta_1\beta_2 + \Xi_{21}(\zeta)\beta_2\beta_1\right]\Big|_{\zeta=\zeta_g}\right\}. \tag{37}$$

The second line of Eq. (36b) represents the virtual cloud of the electron field in the dressed ground state $|\phi_0\rangle$.

IV. ELECTRONIC CASIMIR EFFECT

Now we show the electronic Casimir effect in our system. In this work we consider a symmetric case where

$$\zeta_1 = \zeta_2 = \zeta_0, \quad g_1 = g_2 = g, \tag{38}$$

which leads to

$$\beta_1 = \beta_2 = \frac{1}{\sqrt{2}}. \tag{39}$$

In this case, the characteristic equation of Eq. (35) is factorized as

$$[\zeta_g - \Xi_{11}(\zeta_g) - \Xi_{12}(\zeta_g)][\zeta_g - \Xi_{11}(\zeta_g) + \Xi_{12}(\zeta_0)] = 0. \tag{40}$$

The dressed ground state must appear below the band edge $\zeta_g < 0$.

Taking into account that for $\zeta_g < 0$,

$$\mathrm{Re}\Xi_{11}(\zeta_g) < 0, \quad \mathrm{Re}\Xi_{12}(\zeta_g) < 0, \tag{41a}$$

$$\mathrm{Im}\Xi_{11}(\zeta_g) = \mathrm{Im}\Xi_{12}(\zeta_g) = 0, \tag{41b}$$

the ground-state energy is obtained by solving

$$\zeta_g = \Xi_{11}(\zeta_g) + \Xi_{12}(\zeta_g). \tag{42}$$

Using Eqs. (28) and (29), Eq. (42) reduces to a transcendental equation as

$$\zeta_g - \zeta_0 = -\frac{\pi g^2 u^2}{\sqrt{-\zeta_g}}(1 + e^{-\sqrt{-\zeta_g}R}). \tag{43}$$

In Appendix B we show that the integrals in Eqs. (29) are attributed to the branch point effect of the self-energies and follow the exponential decay in contrast to the electromagnetic case, where they follow a power law decay. In Appendix B we also show that this difference in the distance dependence of the Casimir force originates from the different energy dispersion of the field in the two cases. The dressed ground-state energy is obtained as a function of R and ζ_0 from Eq. (43):

$$\zeta_g = \zeta_g(R;\zeta_0). \tag{44}$$

The right-hand side of Eq. (43) is a self-energy correction to the bare impurity energy, where the second term vanishes in the limit $R \to \infty$, while the first term remains constant. In this limit,

$$\lim_{R\to\infty} \zeta_g(R;\zeta_0) = \zeta_{sg}, \tag{45}$$

where ζ_{sg} is the single-impurity ground-state energy given as a solution of

$$\zeta_{sg} - \zeta_0 = -\frac{\pi g^2 u^2}{\sqrt{-\zeta_{sg}}}. \tag{46}$$

The ground-state energy $\zeta_g(R;\zeta_0)$ is represented as an intersection of the left-hand side and the right-hand side of Eq. (43), which are shown in Fig. 3 by the dotted and solid lines, respectively, with $R = 10$ and $g = 0.1$.

It is found that the ground-state energy $\zeta_g(R;\zeta_0)$ always appears below the band edge for any value of ζ_0 due to the Van Hove singularity. Then we call this bound state a persistent bound state (PBS) which cannot be obtained by the perturbation method from the bare impurity state. Indeed, the

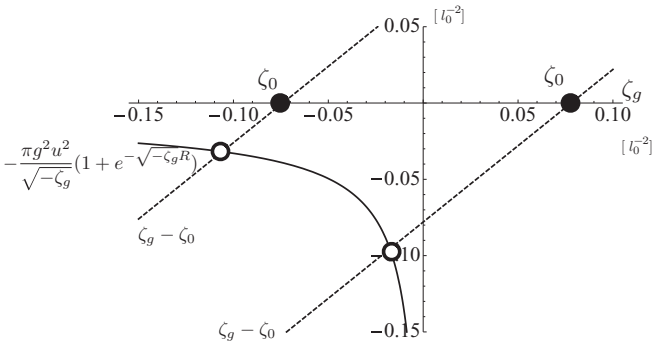

FIG. 3. Characteristic relation for $R = 10$ with $g = 0.1$, where l_0 is a length unit given in Eq. (23).

self-energy shift $|\zeta_g - \zeta_0|$ is much larger than the strength of the interaction $(gv)^2 = 0.01$ as shown in Fig. 3. The appearance of the PBS is a major consequence of Van Hove singularity of the one-dimensional electronic band. In Fig. 4 we show ζ_g as a function of ζ_0 for several values of R: $R = 1$ (solid line), $R = 5$ (dashed line), and $R = 10$ (dotted line), along with the single impurity ground-state energy ζ_{sg} drawn by the thin line.

We define the Casimir energy as the energy difference between ζ_g and ζ_{sg}:

$$\zeta_C(R;\zeta_0) \equiv \zeta_g(R;\zeta_0) - \zeta_{sg}. \tag{47}$$

The Casimir force is then obtained by the negative derivative of $\zeta_C(R;\zeta_0)$ with respect to R:

$$F_C(R;\zeta_0) \equiv -\frac{\partial}{\partial R}\zeta_C(R;\zeta_0). \tag{48}$$

In Fig. 5 we show a log plot of $F_C(R;\zeta_0)$ as a function of R for $\zeta_0 = -0.5$ (solid line), $\zeta_0 = 0$ (long dashed line), $\zeta_0 = 0.5$ (short dashed line), and $\zeta_0 = 1.0$ (dotted line). The R dependence of the Casimir force is changed at $R \simeq R_c \equiv 1/\sqrt{-\zeta_{sg}}$: For $R \gtrsim R_c$, which we call a long regime, the Casimir force decreases exponentially with a decay rate given by $\sqrt{-\zeta_{sg}}$, while it deviates from the exponential law for $R \lesssim R_c$, which we call a short regime. In Fig. 5 R_c is evaluated

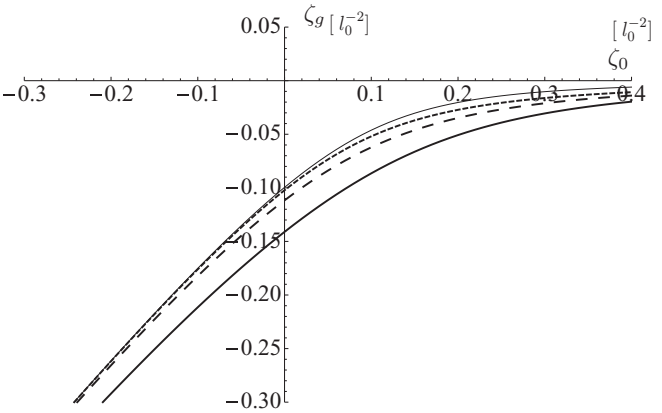

FIG. 4. Ground-state energy ζ_g as a function of ζ_0 for $R = 1$ (solid line), $R = 5$ (dashed line), $R = 10$ (dotted line), and ζ_{sg} (thin line). The length unit is given by Eq. (23).

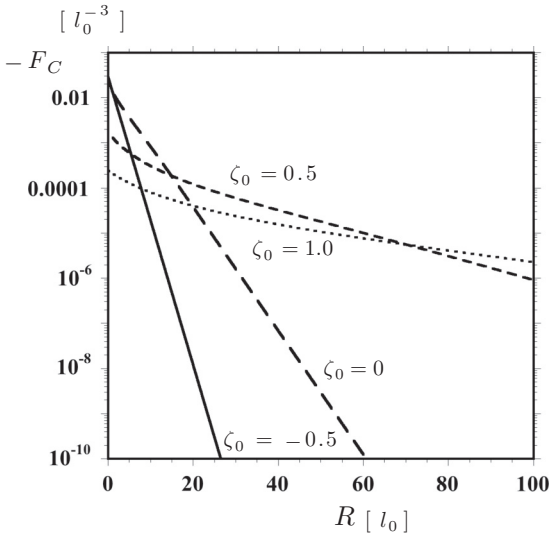

FIG. 5. A log plot of Casimir force for the ground state as a function of R for $\zeta_0 = -0.5$ (solid line), $\zeta_0 = 0$ (long dashed line), $\zeta_0 = 0.5$ (short dashed line), and $\zeta_0 = 1.0$ (dotted line). The critical values R_c are 1.36, 3.17, 16.0, and 31.9 for $\zeta_0 = -0.5$, 0, 0.5, and 1.0, respectively. In the case of adsorbed atom on a silicon semiconductor, the length unit of l_0 is evaluated to be 4.9 Å.

as $R_c = 1.36$, 3.17, 16.0, and 31.9 for $\zeta_0 = -0.5$, 0, 0.5, and 1.0, respectively.

In the long-distance regime, by expanding ζ_g around ζ_{sg} in Eq. (43), the distance dependence of the Casimir energy is approximated by

$$\zeta_C(R;\zeta_0) \simeq -\frac{\frac{\pi g^2 u^2}{\sqrt{-\zeta_{sg}}}}{1+\frac{\pi g^2 u^2}{2(-\zeta_{sg})^{3/2}}} e^{-\sqrt{-\zeta_{sg}}R} \quad (\text{for } R \gtrsim R_c), \tag{49}$$

leading to

$$F_C(R;\zeta_0) \simeq -\frac{\pi g^2 u^2}{1+\frac{\pi g^2 u^2}{2(-\zeta_{sg})^{3/2}}} e^{-\sqrt{-\zeta_{sg}}R} \quad (\text{for } R \gtrsim R_c). \tag{50}$$

The exponential decay is a characteristic feature of a Casimir force due to a massive quantum field, such as a meson field, responsible for the Yukawa force [6]. The decay rate of the Yukawa force is the Compton wavelength of a meson particle $\hbar/mc \simeq 10^{-14}$ m. Contrarily to the short-range nuclear force, the present electronic Casimir force can be of very long range for large ζ_0, as shown in Fig. 5. This is because, as ζ_0 increases, the dressed ground state is obtained as a nonperturbative PBS, so that the decay rate $\sqrt{-\zeta_{sg}}$ becomes small as mentioned above. In Sec. V we shall discuss the effective mass of the present case which determines the exponential decay rate. With use of the length unit evaluated at the end of Sec. II, we can find out that for the case of adsorbed atom on a silicon semiconductor, the decay rate is evaluated as $1/78.4$ Å^{-1} for $\zeta_0 = 0.5$ and $1/156$ Å^{-1} for $\zeta_0 = 1.0$. This means that the covalent bonding between the adsorbed atoms on a one-dimensional silicon surface is enhanced by the charge transfer through the one-dimensional conduction band.

On the other hand, for $R \lesssim R_c$, the distance dependence of the Casimir force differs from the exponential decay. In this

case, we approximate Eq. (43) as

$$\zeta_g - \zeta_0 = -\frac{\pi g^2 u^2}{\sqrt{-\zeta_g}}\left[1 + \sum_{n=0}^{n_c} \frac{1}{n!}(-\sqrt{-\zeta_g}R)^n\right], \tag{51}$$

where the upper limit of the sum n_c is taken to be a large integer so that

$$(\sqrt{-\zeta_g}R)^{n_c} \ll 1 \ \text{ or } \ \left(\frac{R}{R_c}\right)^{n_c} \ll 1. \tag{52}$$

In this case $\sqrt{-\zeta_g}$ is obtained as the lowest solution of the n_c-order polynomial equation. As a result, the Casimir force differs from the exponential law.

The difference of the R dependence of the Casimir force at R_c reminds us the R dependence of the van der Waals–Casimir-Polder force between two atoms as shown in Appendix B where the R dependence as a power law becomes different at a wavelength corresponding to an atomic transition wave number. However, it should be noted that the van der Waals force is evaluated within a perturbation method, while the nonexponential decay in the short regime of the present system is due to a nonperturbative effect.

The long-range character of the electronic Casimir force for the PBS is well reflected in a long tail of the virtual cloud of the field. With use of Eq. (7), the spatial extension of the dressing field is given by

$$\langle x|\phi_0\rangle = \mathcal{N}_0^{1/2}\frac{gu}{\sqrt{\Omega}}\sum_k \frac{1+e^{ikR}}{\sqrt{2L}}\frac{e^{ikx}}{\zeta_g - \zeta_k} \tag{53a}$$

$$= \mathcal{N}_0^{1/2}\frac{gu}{\sqrt{2\pi}}\int_{-\infty}^{\infty} dk \frac{1+e^{ikR}}{\sqrt{2}}\frac{e^{ikx}}{\zeta_g - \zeta_k} \tag{53b}$$

$$= -\mathcal{N}_0^{1/2}\frac{\sqrt{\pi}}{2}\frac{gu}{\sqrt{-\zeta_g}}(e^{-\sqrt{-\zeta_g}|x|} + e^{-\sqrt{-\zeta_g}|x-R|}), \tag{53c}$$

where the normalization constant is obtained by Eqs. (28), (29), (37), and (39) as

$$\mathcal{N}_0^{-1} = 1 - \frac{\partial}{\partial\zeta}[\Xi_{11}(\zeta) + \Xi_{12}(\zeta)]|_{\zeta=\zeta_g} \tag{54a}$$

$$= 1 + \frac{\pi g^2 u^2}{2}\left\{\frac{1}{|\zeta_g|^{3/2}} + \frac{e^{-\sqrt{|\zeta_g|}R}}{|\zeta_g|}\left(R + \frac{1}{|\zeta_g|^{1/2}}\right)\right\}. \tag{54b}$$

In Fig. 6(a) we show the intensity of the virtual cloud $|\langle x|\phi_0\rangle|^2$ for the cases $\zeta_0 = -0.5$ (solid line), $\zeta_0 = 0$ (long dashed line), $\zeta_0 = 0.5$ (short dashed line), and $\zeta_0 = 1.0$ (dotted line), where the two sources are located at $R = 0$ and $R = 20$. When ζ_0 is far below the band edge ($\zeta_0 = -0.5$), the virtual cloud is well localized around the sources and the overlap of the clouds is very small. On the other hand, as ζ_0 increases across the band edge, the virtual cloud is extended far from the impurities and there is a large overlap between the clouds centered at the sources. Because of this long extension of the virtual cloud of the PBS, the electronic Casimir force is effective even at a large distance.

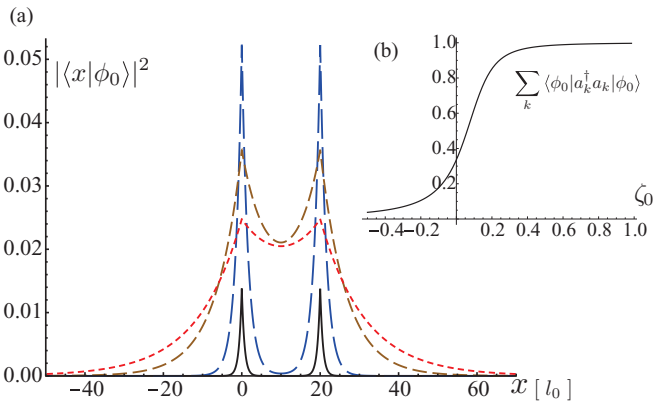

FIG. 6. (Color online) (a) The intensity of the virtual cloud $|\langle x|\phi_0\rangle|^2$ for $\zeta_0 = -0.5$ (solid line), $\zeta_0 = 0$ (long dashed line), $\zeta_0 = 0.5$ (short dashed line), and $\zeta_0 = 1.0$ (dotted line). (b) The number of the virtual quanta of the dressed electron as a function of ζ_0.

V. DISCUSSION

We have shown so far that the electronic Casimir-Polder effect is caused by an overlap of the virtual clouds of the electron field. In this section we shall show that the electronic Casimir-Polder effect can be interpreted by the radiation reaction field [6,7,24]. In the idea of the radiation reaction, one of the two sources creates a virtual cloud of the field around itself, and the interaction of this field with the other atom induces the Casimir-Polder energy which is the origin of the Casimir-Polder force [7].

In the present case we first consider a dressed state of a single impurity at $x = 0$ described by

$$|\phi_s^1\rangle = \mathcal{N}_s^{1/2}\left\{|d_1;0\rangle + \frac{g}{\sqrt{\Omega}}\sum_k \frac{u}{\zeta_{sg} - \zeta_k}|0;k\rangle\right\}, \tag{55}$$

where

$$\mathcal{N}_s^{-1} = 1 + \frac{\pi g^2 u^2}{2|\zeta_{sg}|^{3/2}}. \tag{56}$$

The second term of Eq. (55) describes the virtual cloud of the field around the impurity atom at $x = 0$. The tail of the cloud extends to the position where the other dressed atom is located at $x = R$, which is described by

$$|\phi_s^2\rangle = \mathcal{N}_s^{1/2}\left\{|d_2;0\rangle + \frac{g}{\sqrt{\Omega}}\sum_k \frac{ue^{ikR}}{\zeta_{sg} - \zeta_k}|0;k\rangle\right\}. \tag{57}$$

The virtual cloud of the first dressed atom interacts with the second dressed atom, and the interaction energy is evaluated by

$$\zeta_{RR} = \langle\phi_s^2|g\tilde{V}_2|\phi_s^1\rangle \tag{58a}$$

$$= \mathcal{N}_s\langle d_2;0|g\tilde{V}_2|\left\{\frac{gu}{\sqrt{\Omega}}\sum_k \frac{1}{\zeta_{sg} - \zeta_k}|0;k\rangle\right\} \tag{58b}$$

$$= \mathcal{N}_s\frac{g^2u^2}{\Omega}\sum_k \frac{e^{ikR}}{\zeta_{sg} - \zeta_k} \tag{58c}$$

$$= \mathcal{N}_s\Xi_{12}(\zeta_{sg}). \tag{58d}$$

In the equations above, ζ_{RR} is obtained from the interaction Hamiltonian of atom 2 with the electron field, evaluated between the states corresponding to the dressing cloud of atom 1 and the bare state of atom 2. Since ζ_{RR} coincides with $\zeta_C(R;\zeta_0)$ given by Eq. (49) in the long-distance regime, the electronic Casimir effect in the long-distance regime can be interpreted in line with the idea of the radiation reaction field.

Let us show that the ordering of the fermion operators of the field plays an important role in the evaluation of $\langle\phi_s^2|g\tilde{V}_2|\phi_s^1\rangle$ given by Eqs. (58). For that purpose we represent the dressed states of Eqs. (55) and (57) in terms of the new fermion operators given by

$$\tilde{d}_1^\dagger \equiv \mathcal{N}_s^{1/2}\left(d_1^\dagger + \frac{gu}{\sqrt{\Omega}}\sum_k \frac{1}{\zeta_{sg}-\zeta_k}a_k^\dagger\right), \tag{59a}$$

$$\tilde{d}_2^\dagger \equiv \mathcal{N}_s^{1/2}\left(d_2^\dagger + \frac{gu}{\sqrt{\Omega}}\sum_k \frac{e^{ikR}}{\zeta_{sg}-\zeta_k}a_k^\dagger\right). \tag{59b}$$

The dressed states are then represented by

$$|\phi_s^1\rangle = \tilde{d}_1^\dagger|0;\{0\}\rangle, \quad |\phi_s^2\rangle = \tilde{d}_2^\dagger|0;\{0\}\rangle. \tag{60}$$

Therefore Eqs. (58) is represented by

$$\zeta_{RR} = \langle 0;\{0\}|\tilde{d}_2 g\tilde{V}_2\tilde{d}_1^\dagger|0;\{0\}\rangle \tag{61a}$$

$$= \mathcal{N}_s\frac{g^2u^2}{\Omega}\sum_k \frac{e^{ikR}}{\zeta_{sg}-\zeta_k}\langle\{0\}|a_k a_k^\dagger|\{0\}\rangle \tag{61b}$$

$$= \mathcal{N}_s\,\Xi(\zeta_{sg}). \tag{61c}$$

Equation (61b) indicates that the antinormal ordering of the field operators is attributed to the Casimir energy, suggesting that the vacuum fluctuations also plays a role [7].

Here we would like to make a comment on a critical difference of the vacuum fluctuations in the cases of a fermion and a boson field. Note that a fermion field operator follows anticommutation relations, while a boson field operator follows commutation relations. It is possible to translate a creation and annihilation boson operator into a Fourier component of a classical field, since we can correspond the commutation relation of the boson field to a Poisson bracket of the classical field as normal modes [13,34]. As a result, Casimir effect for a classical field can be interpreted by a radiation reaction, or a overlap of virtual clouds, in the same way as for a quantum boson field, while vacuum fluctuations do not exist in classical Casimir effects.

In the fermion case, however, we cannot discuss the Casimir effect in terms of a classical field because there is no correspondence between the anticommutation relation and Poisson bracket. Therefore, we can see that the vacuum fluctuations of the electronic field have a role in the electronic Casimir effect as mentioned above.

In the preceding section below Eq. (50) we have made a comment on the resemblance of the exponential decay of the electronic Casimir force with a Yukawa force due to the meson field. While the decay rate of the Yukawa force is determined by the fixed value of the meson mass, the decay rate of the electronic Casimir force is changed with the bare impurity energy. Here we shall discuss the effective mass of the present case which determines the exponential decay rate.

For that purpose let us introduce an effective massive fermion field whose Hamiltonian is described by

$$\tilde{H}_F^{\rm eff} = \sum_k \tilde{\zeta}_k\tilde{a}_k^\dagger\tilde{a}_k + \frac{gu}{\sqrt{\Omega}}\sum_k(\gamma_k\tilde{a}_k + \gamma_k^*\tilde{a}_k^\dagger), \tag{62}$$

where the effective massive fermion field operators $\tilde{a}_k$ and $\tilde{a}_k^\dagger$ satisfy the anticommutation relation as

$$\{\tilde{a}_k,\tilde{a}_{k'}^\dagger\} = \delta_{k,k'}, \quad \{\tilde{a}_k,\tilde{a}_{k'}\} = \{\tilde{a}_k^\dagger,\tilde{a}_{k'}^\dagger\} = 0, \tag{63}$$

and have the spectrum

$$\tilde{\zeta}_k \equiv \zeta_{sg} + \zeta_k. \tag{64}$$

The second term in (62) represents the interaction with the sources, which gives a boundary condition onto the effective field. The coupling constants depend on the position of the sources as

$$\gamma_k \equiv \sqrt{\frac{\mathcal{N}_s}{2}}(1+e^{ikR}), \quad \gamma_k^* \equiv \sqrt{\frac{\mathcal{N}_s}{2}}(1+e^{-ikR}). \tag{65}$$

We take an *ansatz* for the dressed vacuum state under the weak coupling condition as

$$|\Phi_G\rangle = \chi_0|0\rangle_F + \sum_k \chi_k a_k^\dagger|0\rangle_F, \tag{66}$$

where the bare vacuum state of the field satisfies

$$\tilde{a}_k|0\rangle_F = 0, \quad \text{for} \quad \forall k, \tag{67}$$

with the bare vacuum energy $E_0 = 0$. The interacting vacuum energy is then obtained by a second-order perturbation theory as

$$E_G \simeq -\frac{g^2u^2}{\Omega}\sum_k \frac{|\gamma_k|^2}{\tilde{\zeta}_k} \tag{68a}$$

$$= -\frac{g^2u^2}{\Omega}\sum_k \frac{1+e^{ikR}}{\zeta_{sg}+\tilde{\zeta}_k} \tag{68b}$$

$$= -g^2u^2\int dk\,\frac{1+e^{ikR}}{\zeta_{sg}+\tilde{\zeta}_k}, \tag{68c}$$

which yields the same Casimir force in the long-distance regime as given by Eq. (50). We have shown in Appendix C that the field Hamiltonian is exactly diagnonalized and that the interacting vacuum energy gives the same results as the above in the weak coupling case.

We notice that the effective field Hamiltonian (62) takes the same form as the meson field Hamiltonian interacting with two separate sources, leading to the nuclear force described by Yukawa potential as

$$V(\mathbf{R}) = -\frac{g}{4\pi c}\frac{e^{-\kappa R}}{R}, \tag{69}$$

where the decay rate is $\kappa \equiv mc/\hbar$ [7]. Thus we may compare our effective field with a relativistic scalar field. By comparison of $\tilde{\varepsilon}_k$ given by Eq. (64) with the spectrum of a meson field

$$\hbar\omega_k = \hbar c\sqrt{\kappa^2+k^2} \simeq \hbar c\kappa\left(1+\frac{k^2}{2\kappa^2}\right), \quad \text{for} \quad \frac{k}{\kappa} \ll 1, \tag{70}$$

we can find that ζ_{sg} of Eq. (64) corresponds to the rest energy $\hbar c\kappa$ of the relativistic scalar field. This means that, by injection

of energy beyond the energy gap $|\zeta_{sg}|$, a field particle is created in the conduction band.

This shows that the energy gap in the electronic Casimir effect leads to a finite effective mass that leads to the exponentially decaying virtual cloud surrounding the atomic particle. This is a striking contrast in the case of the photon, since the virtual cloud of the photon surrounding exchange decay in the power law because the rest mass is zero.

VI. CONCLUDING REMARKS

In this work we have presented the electronic Casimir effect for a system consisting of two impurities on a one-dimensional semiconductor. Due to the charge transfer from the impurity to one-dimensional conduction band, the impurity states are dressed by a virtual cloud of the electron field. The attractive electronic Casimir force arises due to the overlap of the virtual clouds. The Van Hove singularity causes the persistent bound state to appear below the band edge even when the bare impurity state energy is above the band edge. Since the virtual cloud of the PBS extends to a long distance, the Casimir force can be very of long range, even with its exponential decay. It is found that the spatial extension of the electronic Casimir force of an adsorbed atom on the silicon semiconductor reaches to a few hundred Angstrom. Therefore the covalent bonding of the adsorbed atoms on the semiconductor surface is strongly enhanced by the charge transfer via a one-dimensional conduction band.

The electronic Casimir-Polder effect can be interpreted in terms of the radiation reaction field, where one of the two sources creates a virtual cloud of the field around itself, and the interaction of this field with the other atom induces the Casimir-Polder energy which is the origin of the Casimir-Polder force. The difference of the vacuum fluctuations of the boson field and fermion field has been discussed by noticing a correspondence between the commutation relation and Poisson bracket.

We have introduced an effective massive fermion field whose mass is given by the energy gap between the bound state and the band edge of the conduction band. This gives a new insight to the effective mass which is different from an effective band mass of the conduction band.

Recently several sophisticated experimental methods have been developed to observe the Casimir-Polder effect [4,35]. These methods can be also used to detect the electronic Casimir-Polder effect. We think that one of the possible experiments to detect the electronic Casimir-Polder effect is to measure the change of their oscillation frequency of the impurities around their equilibrium positions due to the Casimir-Polder force. Indeed, such an oscillation frequency change has been recently used to detect the Casimir-Polder force between a condensate and a surface under nonequilibrium conditions [36].

In this paper we have focused on a homopolar system in which two adaptors are identical. In the case of a heteropolar adsorbed molecule, such as NaI shown in Fig. 1(b), the ionic bonding effect should be taken into account. However, in a long distance, the covalent boding is important in the ground state instead of the ionic bonding effect as seen in an adiabatic potential curve of a NaI molecule [37]. Furthermore, when the molecule is absorbed on a surface of a condensed matter, the ionic bonding effect is screened out and less important, while the covalent bonding due to the charge transfer through the semiconductor conduction band becomes more important. In our work we focus on the electronic Casimir-Polder effect in such a long distance that the ionic bonding does not play a major role.

In the case of a homopolar molecule, such as an adsorbed H_2 molecule [38,39], we have to take into account Coulomb repulsion of two electrons, which can be incorporated in our model Hamiltonian and may modify the electronic levels of the system. However, since the electronic wave function is extended over in the semiconductor, the Coulomb interaction between the two electrons becomes suppressed. As a result, the ground-state function of the two electron system is approximated well to be a simple direct product of $|\phi_0\rangle$ with opposite spins, resulting in the long-range electronic Casimir-Polder effect in this work.

ACKNOWLEDGMENTS

The authors thank K. Kanki, N. Hatano, G. Ordonez, S. Garmon, L. Rizzuto, and S. Spagnolo for fruitful discussions. This work was supported by the Grant-in-Aid for Scientific Research from the Ministry of Education, Science, Sports, and Culture of Japan. Financial support by the Julian Schwinger Foundation, by Ministero dell'Istruzione, dell'Università e della Ricerca, by Comitato Regionale di Ricerche Nucleari e di Struttura della Materia, and by the ESF Research Networking Program CASIMIR is gratefully acknowledged.

APPENDIX A: BRILLOUIN-WIGNER-FESCHBACH'S PROJECTION METHOD FOR THE EIGENVALUE PROBLEM OF A MULTILEVEL FRIEDRICHS MODEL

In this Appendix we solve the eigenvalue problem of a multidiscrete level Friedrichs model. We solve the eigenvalue problem of a Hamiltonian given by

$$H = H_0 + gV, \tag{A1}$$

where

$$H_0 = \sum_{j=1}^{N} \varepsilon_j |d_j\rangle\langle d_j| + \sum_k \varepsilon_k |k\rangle\langle k|, \tag{A2a}$$

$$gV = \frac{g}{\sqrt{\Omega}} \sum_k \sum_{j=1}^{N} (v_{jk}|d_j\rangle\langle k| + v_{jk}^*|k\rangle\langle d_j|). \tag{A2b}$$

In Eqs. (A2) $|d_j\rangle$ denotes bare discrete states with energy ε_j, and $|k\rangle$ denotes continuous states with energy ε_k. N is the number of discrete states.

Taking into account the situation where the resonant state appears by a resonance, we consider the complex eigenvalue problem of H in extended Hilbert space [30]. We consider the following right- and left-eigenvalue problems:

$$H|\phi_j\rangle = z_j|\phi_j\rangle, \quad \langle\tilde{\phi}_j|H = z_j\langle\tilde{\phi}_j|, \quad \text{for} \quad j = 1\text{–}N, \tag{A3}$$

for the discrete states, and

$$H|\phi_k\rangle = z_k|\phi_k\rangle, \quad \langle\tilde{\phi}_k|H = z_k\langle\tilde{\phi}_k|, \tag{A4}$$

for the continuous field.

In this paper we focus on the discrete states because we want to investigate the Casimir effect of the dressed ground state. Therefore, we consider the projection operators onto the bare discrete states and its complement as

$$\hat{P}^{(d)} \equiv \sum_{j=1}^{N} |d_j\rangle\langle d_j|, \quad \hat{Q}^{(d)} \equiv 1 - \hat{P}^{(d)}. \tag{A5}$$

Acting $\hat{P}^{(d)}$ and $\hat{Q}^{(d)}$ onto the first equation of Eq. (A3), we have

$$\hat{P}H_0\hat{P}|\phi_j\rangle + \hat{P}gV\hat{Q}|\phi_j\rangle = z_j\hat{P}|\phi_j\rangle, \tag{A6a}$$

$$\hat{Q}gV\hat{P}|\phi_j\rangle + \hat{Q}H\hat{Q}|\phi_j\rangle = z_j\hat{Q}|\phi_j\rangle. \tag{A6b}$$

Hereafter in this Appendix we drop the superscripts in $\hat{P}^{(d)}$ and $\hat{Q}^{(d)}$ for simplicity. From the second equation we have

$$\hat{Q}|\phi_j\rangle = \hat{Q}\hat{C}(z)\hat{P}|\phi_j\rangle, \tag{A7}$$

where

$$\hat{C}(z) \equiv \frac{1}{(z - \hat{Q}H\hat{Q})^{+}}\hat{Q}gV\hat{P}. \tag{A8}$$

Equation (A7) means that the $\hat{Q}$ component is obtained as a functional of the $\hat{P}$ component of $|\phi_j\rangle$. In Eq. (A8) $\hat{C}(z)$ contains a Cauchy integral in the propagator, and the sign $+$ in the denominator implies to take analytic continuation from the upper half plane to the lower half plane [31].

Substituting Eq. (A7) into Eq. (A6a) results in

$$\hat{\Xi}(z_j)\hat{P}|\phi_j\rangle = z_j\hat{P}|\phi_j\rangle, \tag{A9}$$

or extracting the normalization constant $\mathcal{N}_j$ of $|\phi_j\rangle$ from the above Eq. (A9) reduces to

$$\hat{\Xi}(z_j)|u_j\rangle = z_j|u_j\rangle, \tag{A10}$$

where we have defined

$$|u_j\rangle \equiv \mathcal{N}_j^{-1/2}\hat{P}|\phi_j\rangle. \tag{A11}$$

In Eq. (A9) or (A10) $\hat{\Xi}_c(z)$ is a self-energy operator given by

$$\hat{\Xi}(z) = \hat{P}H_0\hat{P} + \hat{\mathcal{P}}gV\hat{Q}\frac{1}{(z - \hat{Q}H\hat{Q})^{+}}\hat{Q}gV\hat{P}, \tag{A12}$$

where the $+$ sign in the denominator determines the direction of the analytic continuation of a Cauchy integral which appears in the propagator. It should be noted that $\hat{\Xi}(z)$ acts as a operator in the N-discrete state vector subspace. This is an analog of a collision operator in Liouville space [31].

In order to obtain the $\hat{P}$ component of $|\phi_j\rangle$, we solve the nonlinear eigenvalue problem of $\hat{\Xi}$ in a discrete state subspace of $\{|d_j\rangle\}$.

Taking into account Eq. (A7), the discrete eigenstates of H is then given by

$$|\phi_j\rangle = \mathcal{N}_j^{1/2}[|u_j\rangle + \hat{Q}\hat{C}(z_j)|u_j\rangle]. \tag{A13}$$

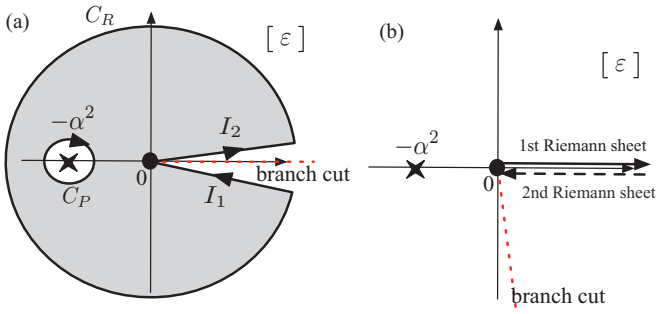

FIG. 7. (Color online) A contour in the energy space. Contour goes along the first and second Riemann sheet.

APPENDIX B: BRANCH POINT EFFECT OF THE SELF-ENERGIES

In this Appendix we study the integral in Eq. (29):

$$I(z) \equiv \int_{-\infty}^{\infty} \frac{e^{ikR}}{k^2 - \tilde{z}_+}dk, \tag{B1}$$

where $\tilde{z} \equiv 2m_e z/\hbar^2$ and the $+$ sign means to place z in the upper half complex plane. In this work we are concentrated to the region of $\mathrm{Re}[z] < 0$ and $\mathrm{Im}[z] = 0$, and we consider

$$\int_{-\infty}^{\infty} \frac{\exp(ikx)}{\alpha^2 + k^2}dk \quad (\text{for } \alpha > 0), \tag{B2}$$

where $\alpha \equiv -\mathrm{Re}[z]$. Here we rewrite this with use of the energy variable ε defined by

$$\varepsilon \equiv k^2, \quad \text{i.e.,} \quad k = \sqrt{\varepsilon}. \tag{B3}$$

Here we have to notice that $\sqrt{\varepsilon}$ is a two-valued function with a singularity at $\varepsilon = 0$, which forces us to use the second Riemann sheet to consider the integral. In Fig. 7 we show the branch cut in the complex ε plane, where we take a branch cut depicted by a broken line.

So we divide the integral (B2) into two parts as

$$\int_{-\infty}^{\infty} \frac{\exp(ikx)}{\alpha^2 + k^2}dk = \int_{-\infty}^{0} \frac{\exp(ikx)}{\alpha^2 + k^2}dk + \int_{0}^{\infty} \frac{\exp(ikx)}{\alpha^2 + k^2}dk \equiv I_1 + I_2. \tag{B4}$$

In I_1, since k is negative, we take $\varepsilon = |k|\exp(i2\pi - i\delta)$, where δ is a positive infinitesimal, while in I_2, since k is positive, we take $\varepsilon = |k|\exp(i\delta)$, as shown in Fig. 7(a) in the ε plane. By taking this contour we change the integral in k plane to ε plane:

$$I_1 = \int_{I_1} \frac{\exp(i\sqrt{\varepsilon}x)}{\alpha^2 + \varepsilon}\frac{d\varepsilon}{2\sqrt{\varepsilon}}, \tag{B5a}$$

$$I_2 = \int_{I_2} \frac{\exp(i\sqrt{\varepsilon}x)}{\alpha^2 + \varepsilon}\frac{d\varepsilon}{2\sqrt{\varepsilon}}. \tag{B5b}$$

When we move the branch cut as shown in Fig. 7(b), it is seen that both the contours of the integrals belong to different Riemann sheets: I_1 and I_2 belong to the first and second Riemann sheets, respectively. Figure 7(b) shows that the integral is attributed to the branch point effect.

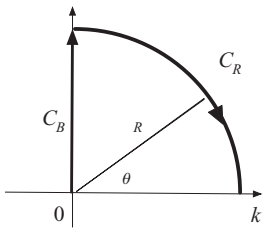

FIG. 8. A deformed contour.

In order to evaluate Eqs. (B5), we consider a closed loop contour as shown in Fig. 7(a) consisting of $I_1 + I_2 + C_R + C_P$. Since $I_1 + I_2 + C_R + C_P = 0$ and $C_R = 0$, we have

$$I_1 + I_2 = -\int_{C_P} \frac{\exp(i\sqrt{\varepsilon}x)}{\alpha^2 + \varepsilon} \frac{d\varepsilon}{2\sqrt{\varepsilon}} \tag{B6a}$$

$$= -(-2\pi i)\,\mathrm{Res}[\varepsilon = -\alpha^2] = \frac{\pi}{\alpha} e^{-\alpha x}, \tag{B6b}$$

where we have used the fact that $\varepsilon = -\alpha^2$ is in the first Riemann sheet, resulting in $\sqrt{-\alpha^2} = \alpha \exp(i\pi/2) = i\alpha$.

Next we compare this result with the electromagnetic case which presents the power law decay due to the branch point effect. We consider the following integral in which we encounter the calculation of the Casimir energy in the electromagnetic case [7]:

$$\int_0^\infty k^n \frac{\exp(ikx)}{k + k_0} dk, \tag{B7}$$

where k_0 represents a wave number corresponding to an atomic transition energy.

First we deform the contour as shown in Fig. 8. The integral along C_R vanishes because this part brings about $\lim_{R\to\infty} \exp(-Rx \sin\theta) = 0$ at the large radius of k. The integral along C_B (branch point contribution) has to be evaluated. For that purpose, we transform the variable as $k = iu$. The integral then becomes

$$\int_0^\infty k^n \frac{\exp(ikx)}{k + k_0} dk = i \int_0^\infty (iu)^n \frac{\exp(-xu)}{iu + k_0} du$$

$$= \int_0^\infty (iu)^n \frac{\exp(-xu)}{u - ik_0} du. \tag{B8}$$

Next we transform the variable u with y as $y = xu$, which leads Eq. (B8) to

$$\int_0^\infty k^n \frac{\exp(ikx)}{k + k_0} dk = i^n \int_0^\infty \left(\frac{y}{x}\right)^n \frac{\exp(-y)}{\frac{y}{x} - ik_0} \frac{dy}{x}$$

$$= \frac{i^n}{x^n} \int_0^\infty \frac{y^n \exp(-y)}{y - ik_0 x} dy. \tag{B9}$$

It is found that the integral has a contribution only within $y \sim 1$ due to the exponential factor. And for a long range of x compared to the atomic transition length $1/k_0$, i.e., far-zone case $1 \ll k_0 x$, Eq. (B9) can be approximated as

$$\int_0^\infty k^n \frac{\exp(ikx)}{k + k_0} dk \simeq \frac{i^{n+1}}{k_0 x^{n+1}} \int_0^\infty y^n \exp(-y) dy$$

$$= \frac{i^{n+1}}{n!\, k_0} \frac{1}{x^{n+1}}. \tag{B10}$$

On the other hand, for the near-zone case $1 \gg k_0 x$, we can evaluate Eq. (B7) as

$$\int_0^\infty k^n \frac{\exp(ikx)}{k + k_0} dk \simeq \frac{i^n}{x^n} \int_0^\infty y^{n-1} \exp(-y) dy$$

$$= \frac{i^n}{(n-1)!} \frac{1}{x^n}. \tag{B11}$$

Equations (B10) and (B11) explain the retardation effect of the van der Waals–Casimir-Polder force which shows x^{-6} and x^{-7} dependence for near and far zone, respectively [7].

APPENDIX C: EXACT DIAGONALIZATION OF THE EFFECTIVE FIELD HAMILTONIAN

The effective field Hamiltonian introduced in Sec. V can be diagonalized if we reorder the operator such that

$$\tilde{H}_F^{\mathrm{eff}} = \sum_k \left\{ \tilde{\zeta}_k \frac{1}{2} (a_k^\dagger a_k - a_k a_k^\dagger) + \gamma_k a_k + \gamma_k^* a_k^\dagger \right\} + \tilde{\zeta}_0$$

$$\equiv \sum_k \tilde{h}_k + \tilde{\zeta}_0, \tag{C1}$$

where

$$\tilde{\zeta}_0 \equiv \frac{1}{2} \sum_k \tilde{\zeta}_k. \tag{C2}$$

The eigenvalue problem of the Hamiltonian of $\tilde{h}_k$ is readily solved as

$$\tilde{h}_k |\varphi_{k\pm}\rangle = \tilde{\zeta}_{k\pm} |\varphi_{k\pm}\rangle, \tag{C3}$$

where the eigenvalues are obtained as

$$\tilde{\zeta}_{k\pm} = \pm \frac{\zeta_k}{2} \sqrt{1 + \frac{4|\gamma_k|^2}{\zeta_k^2}}. \tag{C4}$$

The eigenstates of $\tilde{h}_k$ are given by

$$|\varphi_{k\pm}\rangle = c_{0k\pm} |0_k\rangle + c_{1k\pm} a_k^\dagger |0_k\rangle, \tag{C5}$$

where

$$\frac{c_{0k\pm}}{c_{1k\pm}} = \frac{\zeta_k}{2\gamma_k} \left(1 \pm \sqrt{1 + \frac{4|\gamma_k|^2}{\zeta_k^2}}\right), \tag{C6}$$

with

$$|c_{0k\pm}|^2 + |c_{1k\pm}|^2 = 1. \tag{C7}$$

The field ground state are then given by

$$|\Phi_G\rangle = \prod_k (c_{0k-} |0_k\rangle + c_{1k-} a_k^\dagger |0_k\rangle), \tag{C8}$$

and the ground-state energy of the field is given by

$$\zeta_G = \zeta_0 + \sum_k \tilde{\zeta}_{k-} = \sum_k \frac{\zeta_k}{2} - \sum_k \frac{\zeta_k}{2}\sqrt{1 + \frac{4|\gamma_k|^2}{\zeta_k^2}}. \tag{C9}$$

In the weak coupling case ζ_G is approximated by

$$\zeta_G \simeq \sum_k \frac{\zeta_k}{2} - \sum_k \frac{\zeta_k}{2}\left(1 + \frac{2|\gamma_k|^2}{\zeta_k^2}\right) \tag{C10a}$$

$$= -\frac{g^2u^2}{\Omega}\sum_k \frac{1 + e^{ikR}}{\zeta_{sg} + k^2} \tag{C10b}$$

$$= -g^2u^2 \int dk \frac{1 + e^{ikR}}{\zeta_{sg} + k^2}\,, \tag{C10c}$$

which yields the Casimir force in the long regime given by Eq. (50).

[1] H. B. G. Casimir and D. Polder, Phys. Rev. **73**, 360 (1948).
[2] M. Bordag, G. L. Klimchitskaya, U. Mohideen, and V. M. Mostepanenko, *Advances in the Casimir Effect* (Oxford University Press, Oxford, 2009).
[3] D. Dalvit, P. Milonni, D. Roberts, and F. Rosa (Eds.), *Casimir Physics* (Springer, New York, 2011).
[4] S. K. Lamoreaux, Phys. Today **60**, 40 (2007).
[5] B. B. Machta, S. L. Veatch, and J. P. Sethna, Phys. Rev. Lett. **109**, 138101 (2012).
[6] P. W. Milonni, *The Quantum Vacuum* (Academic, New York, 1994).
[7] G. Compagno, R. Passante, and F. Persico, *Atom-Field Interactions and Dressed Atoms* (Cambridge University Press, Cambridge, 1995).
[8] S. John and J. Wang, Phys. Rev. Lett. **64**, 2418 (1990).
[9] S. John and T. Quang, Phys. Rev. A **50**, 1764 (1994).
[10] X-H. Wang, Y. S. Kivshar, and B. Y. Gu, Phys. Rev. Lett. **93**, 073901 (2004).
[11] S. Garmon, H. Nakamura, N. Hatano, and T. Petrosky, Phys. Rev. B **80**, 115318 (2009).
[12] S. Tanaka, S. Garmon, and T. Petrosky, Phys. Rev. B **73**, 115340 (2006).
[13] T. Petrosky, G. Ordonez, and I. Prigogine, Phys. Rev. A **68**, 022107 (2003).
[14] G. Barton, Proc. R. Soc. London Ser. A **410**, 141 (1987).
[15] R. Messina, R. Passante, L. Rizzuto, S. Spagnolo, and R. Vasile, J. Phys. A **41**, 164031 (2008).
[16] M. Boström, J. J. Longdell, D. J. Mitchell, and B. W. Ninham, Eur. Phys. J. D **22**, 47 (2003).
[17] H. R. Haakh, J. Schiefele, and C. Henkel, Int. J. Mod. Phys. Conf. Ser. **14**, 347 (2012).
[18] T. Petrosky and I. Prigogine, Physica A **147**, 439 (1988).
[19] S. Y. Buhmann, L. Knöll, D.-G. Welsch, and H. T. Dung, Phys. Rev. A **70**, 052117 (2004).
[20] G. Flores-Hidalgo and A. P. C. Malbouisson, Phys. Rev. A **66**, 042118 (2002).
[21] F. Ciccarello, E. Karpov, and R. Passante, Phys. Rev. A **72**, 052106 (2005).
[22] R. Passante, L. Rizzuto, S. Spagnolo, S. Tanaka, and T. Y. Petrosky, Phys. Rev. A **85**, 062109 (2012).
[23] S. Tanaka, S. Garmon, G. Ordonez, and T. Petrosky, Phys. Rev. B **76**, 153308 (2007).
[24] P. W. Milonni, Phys. Scripta T **21**, 102 (1988).
[25] P. W. Milonni, Phys. Scripta **76**, C167 (2007).
[26] C. Cohen-Tannoudji, J. D.-Roc, and G. Grynberg, *Atom-Photon Interactions* (Wiley-Interscience, New York, 1992).
[27] P. W. Anderson, Phys. Rev. **124**, 41 (1961).
[28] D. M. Newns, Phys. Rev. **178**, 1123 (1969).
[29] A. Messiah, *Quantum Mechanics* (Dover, New York, 1999).
[30] T. Petrosky, I. Prigogine, and S. Tasaki, Physica A **173**, 175 (1991).
[31] T. Petrosky and I. Prigogine, Adv. Chem. Phys. **99**, 1 (1997).
[32] G. Ordonez, T. Petrosky, and I. Prigogine, Phys. Rev. A **63**, 052106 (2001).
[33] T. Petrosky, G. Ordonez, and I. Prigogine, Phys. Rev. A **64**, 062101 (2001).
[34] T. Petrosky, Int. J. Quantum Chem. **98**, 103 (2004).
[35] A. W. Rodriguez, F. Capasso, and S. G. Johnson, Nat. Photon. **5**, 211 (2011).
[36] J. M. Obrecht, R. J. Wild, M. Antezza, L. P. Pitaevskii, S. Stringari, and E. A. Cornell, Phys. Rev. Lett. **98**, 063201 (2007).
[37] A. Mokhtari, P. Cong, J. L. Herek, and A. H. Zewail, Nature (London) **348**, 225 (1990).
[38] M. Durr and U. Hofer, Surf. Sci. Rep. **61**, 465 (2006).
[39] A. M. Wodtke, D. Matsiev, and D. J. Auerbach, Prog. Surf. Sci. **83**, 167 (2008).